

Regioselective Recognition of a [60]Fullerene-Bisadduct by Cyclodextrin

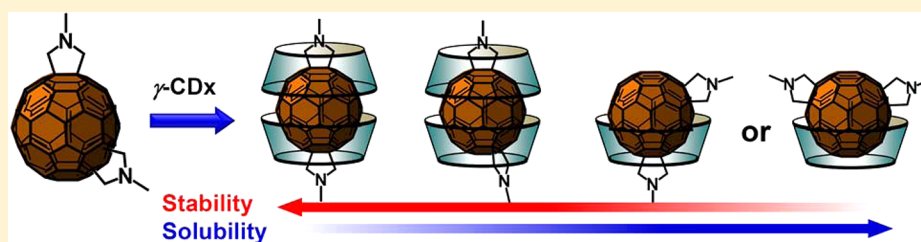
Atsushi Ikeda,^{*,†} Michiko Ishikawa,[†] Ryota Aono,[†] Jun-ichi Kikuchi,[†] Motofusa Akiyama,^{†,‡} and Wataru Shinoda[§]

[†]Graduate School of Materials Science, Nara Institute of Science and Technology, 8916-5 Takayama, Ikoma 630-0192, Japan

[‡]Department of Applied Chemistry, Faculty of Science and Engineering, Chuo University, 1-13-27 Kasuga, Bunkyo-ku, Tokyo 113-8551, Japan

[§]Health Research Institute (HRI), National Institute of Advanced Industrial Science and Technology (AIST), 1-8-31 Midorigaoka, Ikeda 563-8577, Japan

S Supporting Information



ABSTRACT: The three different regioisomers of bis-*N*-methylfulleropyrrolidines have been separated by controlling the relative amounts of γ -cyclodextrin and dimethyl sulfoxide (DMSO) contained in solutions of these compounds. When a small amount of γ -CDx was used in a mechanochemical high-speed vibration milling apparatus, the *trans*-1 and *trans*-2• γ -CDx complexes were separated from the *trans*-3• γ -CDx complex. In contrast, *trans*-3 was extracted in a relatively high ratio with an excess of γ -CDx. The addition of DMSO to aqueous solutions of the fullerene derivative• γ -CDx complexes allowed for the three regioisomers to be obtained in high purity (>95%). The basis for the observed regioselective separation was a competition between the relative stabilities and solubilities of the complexes in the water and water-DMSO solvents. The stabilities of the complexes in water were assessed by the number of hydrogen bonding interactions between the two γ -CDx units using molecular dynamics simulations. To the best of our knowledge, this is the first reported example of the isolation of the different regioisomers of fullerene derivatives using host–guest complexes.

INTRODUCTION

Fullerenes display a wide range of unique electronic and optical properties.¹ To enable the effective application of these properties, organochemical derivatization of C₆₀ is necessary to improve its solubility and overall functionality.² Bisaddition to C₆₀ usually leads to a mixture of regioisomers and the resulting isomers possess different properties. Numerous efforts have been made to purify and isolate regio- and stereochemically pure bisfunctionalized C₆₀ derivatives.³ To date, only two methods have been employed for this purpose, including the separation of the mixtures by high performance liquid chromatography (HPLC)⁴ and the regioselective syntheses of bis-adducts using connectors or protecting groups.^{5,6} In contrast, there have been several reports describing the successful purification of pristine C₆₀,^{7,8} C₇₀,^{8,9} and higher fullerene¹⁰ materials through the formation of host–guest complexes. To the best of our knowledge, however, there have been no reports describing the isolation of the different regioisomers of fullerene derivatives using host–guest complexes.

Fullerenes and their derivatives have been solubilized in water by the addition of solubilizing agents.¹¹ γ -Cyclodextrin (γ -CDx) can form a 2:1 complex with C₆₀ and C₇₀ in water.¹² Furthermore, we recently reported that the pyrrolidine and *N*-acylpyrrolidine derivatives of C₆₀ can be included in γ -CDx.¹³ X-ray crystallographic analysis of an *N*-acylpyrrolidine derivative of C₆₀ showed that it formed a 1:2 complex with γ -CDx that possessed a pseudorotaxane structure in which the *N*-acylated pyrrolidine moiety penetrated the upper rim of either of two γ -CDx units.^{13b} Multiple hydrogen bonding interactions between the two γ -CDx units played a key role in stabilizing the fullerene• γ -CDx 1:2 complex.

Herein, we describe the separation of bis-substituted fullerene derivatives by complexation with γ -CDx. Bis-*N*-methylfulleropyrrolidines (**1**, Figure 1) were selected as the target molecules, because they are precursors of cationic bis-*N,N*-dimethylfulleropyrrolidinium salts, which can act as inhibitors of bacterial and cancer cell growth and the enzymatic

Received: December 19, 2012

Published: February 7, 2013

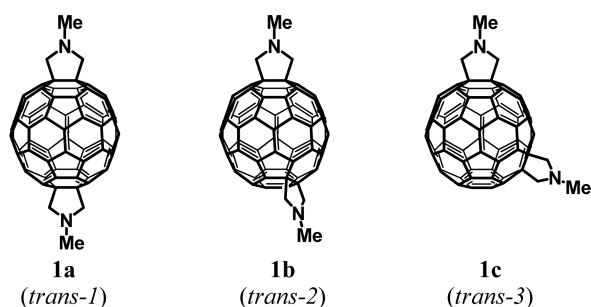


Figure 1. Structures of the three isomers purified from the eight regioisomers of **1** by column chromatography.

activity of acetylcholinesterase. They also possess anti-HIV activity.¹⁴

RESULTS AND DISCUSSION

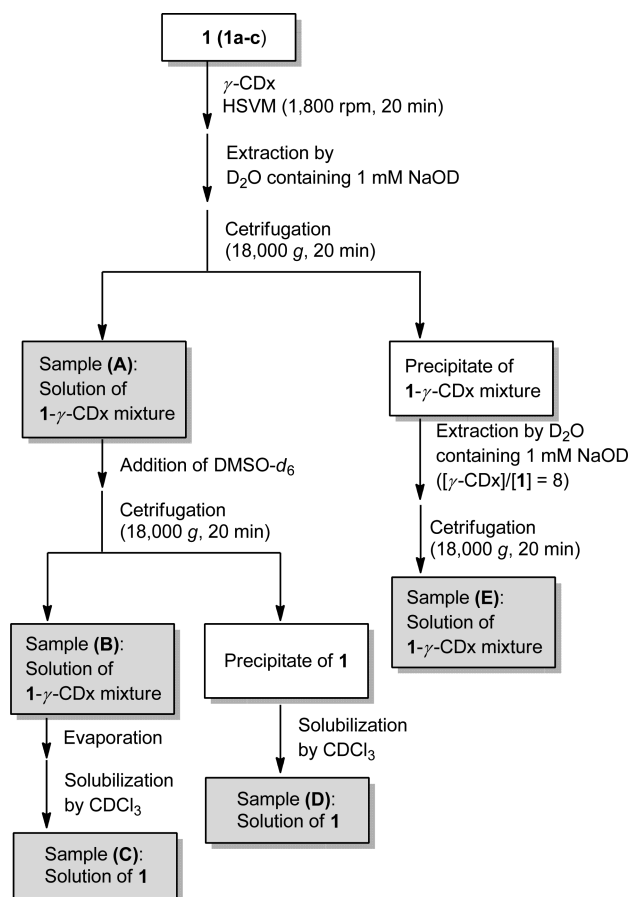
Separation of Three Isomers from a Mixture of Eight Isomers. A mixture consisting of three trans isomers (**1a–c**) was separated from five other isomers by column chromatography on silica gel [Figures 1 and S1, Supporting Information (SI)].^{4e} The isolation of **1a–c** was confirmed by ¹H NMR and mass spectroscopic analyses (Figures S2a and S3, SI). The ¹H NMR spectrum of the original mixture of **1** (prior to HSVM treatment) revealed three distinct *N*-methyl resonances corresponding to the three isomers **1a–c** in a 11:40:49 ratio (Table S1 and Figure S2b, SI).^{4e}

Preparation of 1•γ-CDx Complexes. The **1**•γ-CDx complexes were prepared using a mechanochemical high-speed vibrational milling (HSVM) apparatus according to the method reported by Komatsu (Scheme 1).^{12b,13} Thus, a mixture of **1** and γ-CDx ([γ-CDx]/[**1**] = 1.0, 1.5, 2.0, 4.0, or 8.0) was mixed vigorously using the HSVM apparatus and then dissolved in a D₂O solution containing 1.0 mM NaOD.¹⁵ The resulting brown emulsion was then centrifuged to remove any nondispersed **1**. The regiochemistry of **1** and the formation of the **1**•γ-CDx complexes in the D₂O extract were determined by ¹H NMR spectroscopy [Figure 2; sample (A) in Scheme 1]. The **1**•γ-CDx complexes were then decomposed by the addition of dimethyl sulfoxide (DMSO) to give **1** as a black precipitate. The stoichiometries of the regioisomers in the precipitates were determined by ¹H NMR analysis in CDCl₃ [Figure S4, SI; sample (D) in Scheme 1].^{4e,16}

Ratios of Three Regioisomers in the 1•γ-CDx Complexes. Following the complex formation with γ-CDx in D₂O [sample (A) in Scheme 1], ¹H NMR analysis revealed the ratios of the three regioisomers of **1** to be highly dependent on the amount of γ-CDx present (Table S1, SI, Figures 2b–f, 3, and S4, SI). When a small amount of γ-CDx was used ([γ-CDx]/[**1**] = 1.0 and 1.5), the **1a** and **1b**•γ-CDx complexes could be separated from **1c**•γ-CDx complex ([γ-CDx]/[**1**] = 1.0, **1a**:**1b**:**1c**•γ-CDx complexes = 12:87:1; [γ-CDx]/[**1**] = 1.5, **1a**:**1b**:**1c**•γ-CDx complexes = 13:86:1).

The ratio of the **1c**•γ-CDx complex, however, increased with increasing amounts of γ-CDx ([γ-CDx]/[**1**] = 2.0, **1a**:**1b**:**1c**•γ-CDx complexes = 12:77:12; [γ-CDx]/[**1**] = 4.0, **1a**:**1b**:**1c**•γ-CDx complexes = 7:44:49). It was difficult to separate **1a** and **1b** by complex formation with γ-CDx using the HSVM treatment because the ratios of [**1a**]/[**1b**] (0.14–0.16) remained almost unchanged in a range of [γ-CDx]/[**1**] = 1.0–4.0. Figure 4 shows the UV–vis absorption spectra of the **1**•γ-CDx complexes [sample (A) in Scheme 1]. The solubility

Scheme 1. Schematic Diagram for the Purification of **1** in Water with γ-CDx



of the **1**•γ-CDx complexes in D₂O containing NaOD increased with increasing amounts of γ-CDx up to [γ-CDx]/[**1**] = 2.0, as shown by the absorbance at 250 nm (Figure 4 inset).

In contrast, **1c** could be extracted using a larger amount of γ-CDx ([γ-CDx]/[**1**] = 8.0, **1a**:**1b**:**1c**•γ-CDx complexes = 3:12:86) [Table S1, SI, Figures 2f, 3, and S4e, SI; sample (A) in Scheme 1]. The solubility of **1** in D₂O containing NaOD decreased with increasing amounts of γ-CDx over [γ-CDx]/[**1**] = 2.0, as indicated by the absorbance at 250 nm of [γ-CDx]/[**1**] = 2.0, as indicated by the absorbance at 250 nm of [γ-CDx]/[**1**] (Figure 4 inset). It was therefore envisaged that the dissolution rates of the **1a** and **1b**•γ-CDx complexes could be inhibited by the presence of excess free γ-CDx. To investigate this hypothesis, 6 equiv of γ-CDx were added to a solution of the **1**•γ-CDx complexes that was at [γ-CDx]/[**1**] = 2.0. As shown in Figure 5, precipitation was observed following the addition of γ-CDx. Although the root cause of this precipitation remains unclear, we believe that the precipitation of the **1a** and **1b**•γ-CDx complexes was facilitated by intermolecular complexation with the excess γ-CDx units. It was clear that the majority of the **1a** and **1b**•γ-CDx complexes precipitated and only the **1c**•γ-CDx complex remained in solution because the UV–vis absorption spectrum of the solution (Figure S5, blue line, SI) following the addition of excess CDx units was similar to that of the **1c**•γ-CDx complex (Figure 4, orange line). Furthermore, when [γ-CDx]/[**1**] = 8.0, it was envisaged that the residue obtained following the HSVM treatment would consist of the **1a** and **1b**•γ-CDx complexes. That is, although the **1a** and **1b**•γ-CDx complexes were formed in the residue when [γ-CDx]/[**1**] = 8.0, these complexes were insoluble in D₂O

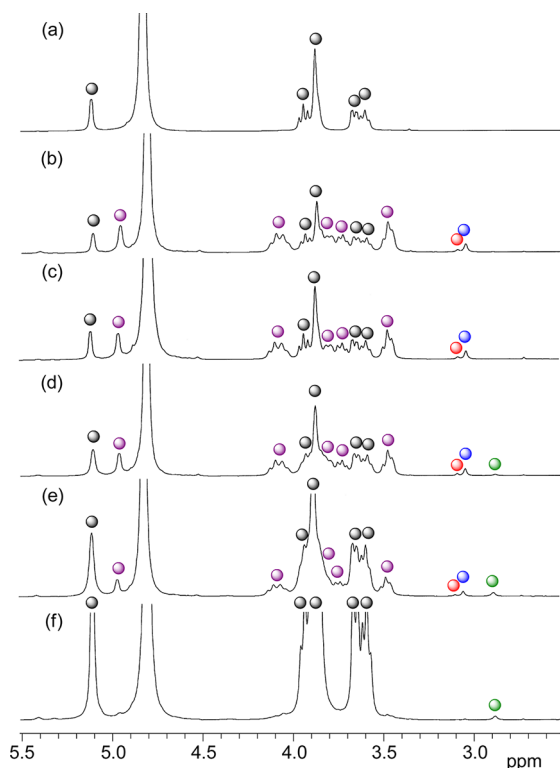


Figure 2. ^1H NMR spectra (400 MHz, D_2O) of $1\text{-}\gamma\text{-CD}_x$ containing 1.0 mM NaOD following HSVM [sample (A) in Scheme 1] at 25 °C. (a) $\gamma\text{-CD}_x$, $[\gamma\text{-CD}_x]/[1] = 1.0$; (b) 1.0, (c) 1.5, (d) 2.0, (e) 4.0, and (f) 8.0. (●, free $\gamma\text{-CD}_x$; purple ●, $\gamma\text{-CD}_x$ in the $1\text{-}\gamma\text{-CD}_x$ complex; red ●, 1a ; blue ●, 1b ; green ●, 1c).

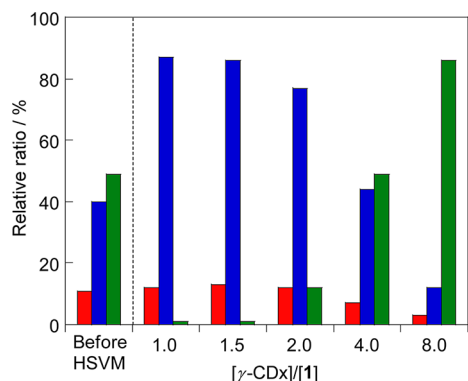


Figure 3. Relative ratios of 1 prior to the HSVM treatment and the ratios of the $1\text{-}\gamma\text{-CD}_x$ complexes in the D_2O solutions following the HSVM treatment with $\gamma\text{-CD}_x$ [sample (A) in Scheme 1]. $[\gamma\text{-CD}_x]/[1] = 1.0, 1.5, 2.0, 4.0,$ and 8.0 (red bar, 1a ; blue bar, 1b ; green bar, 1c).

containing NaOD in the presence of the excess $\gamma\text{-CD}_x$. When $[\gamma\text{-CD}_x]/[1] = 8.0$, the residue was re-extracted with D_2O containing NaOD and the ratio of the three regioisomers in the re-extracted solution was determined by ^1H NMR analysis in D_2O [Figure S6, SI; sample (E) in Scheme 1]. The ratios of the $1\text{a:1b:1c}\text{-}\gamma\text{-CD}_x$ complexes were found to be 11:82:7 (Table S2, SI). In accordance with our prediction, the 1a and $1\text{b}\text{-}\gamma\text{-CD}_x$ complexes had already formed in the residue when $[\gamma\text{-CD}_x]/[1] = 8.0$. Figure S6, SI, shows that the assignable peaks appeared for $\gamma\text{-CD}_x$ in the 1a and $1\text{b}\text{-}\gamma\text{-CD}_x$ complexes.

Purification of the Three Regioisomers by the Addition of DMSO. To obtain the pure 1 being free from

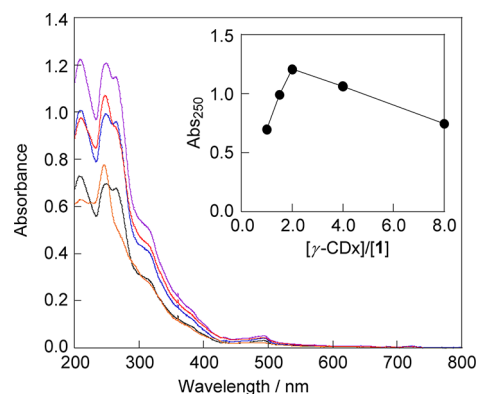


Figure 4. UV-vis absorption spectra of the $1\text{-}\gamma\text{-CD}_x$ complexes in D_2O containing NaOD following the HSVM treatment [sample (A) in Scheme 1]. $[\gamma\text{-CD}_x]/[1] =$ (a) 1.0 (black line), (b) 1.5 (blue line), (c) 2.0 (purple line), (d) 4.0 (red line), and (e) 8.0 (orange line). All spectra were measured at 25 °C (1 mm cell). (Inset) Absorbance at 250 nm.

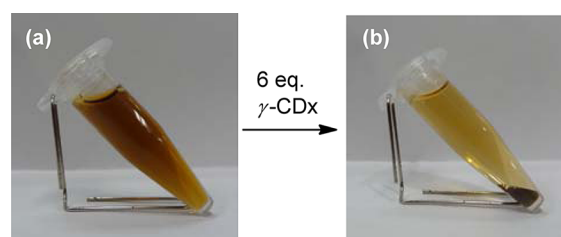


Figure 5. Photographs of the aqueous solutions of the $1\text{-}\gamma\text{-CD}_x$ complex in $[\gamma\text{-CD}_x]/[1] = 2.0$ (a) before and (b) after the addition of 6 equiv of $\gamma\text{-CD}_x$.

$\gamma\text{-CD}_x$, DMSO was added to the D_2O solution of the $1\text{-}\gamma\text{-CD}_x$ complexes. The regiochemistries of 1 in the precipitate were determined by ^1H NMR analysis of the precipitate dissolved in CDCl_3 [Figure 6a–e; sample (D) in Scheme 1]. Under the small amount of $\gamma\text{-CD}_x$ conditions ($[\gamma\text{-CD}_x]/[1] = 1.0$ and 1.5), the ratio of 1b increased with increasing amounts of $\gamma\text{-CD}_x$ ($[\gamma\text{-CD}_x]/[1] = 1.0, 1\text{a:1b:1c} = 7:93:0$; $[\gamma\text{-CD}_x]/[1] = 1.5, 1\text{a:1b:1c} = 4:96:0$) (Table S2, SI, Figures 6a,b and 7). When $[\gamma\text{-CD}_x]/[1] = 1.5$, the proportion of 1a in the $1\text{-}\gamma\text{-CD}_x$ complexes was high in the D_2O – $\text{DMSO-}d_6$ solution [filtrate; sample (B) in Scheme 1] and increased with increasing amounts of $\text{DMSO-}d_6$ [$\text{D}_2\text{O:DMSO-}d_6 = 1:1$ (v/v): $1\text{a:1b:1c}\text{-}\gamma\text{-CD}_x$ complexes = 45:55:0, $\text{D}_2\text{O:DMSO-}d_6 = 2:3$ (v/v): $1\text{a:1b:1c}\text{-}\gamma\text{-CD}_x$ complexes = 95:5:0] (Table S2 and Figure S7b,c, SI). These results indicated that the $1\text{a}\text{-}\gamma\text{-CD}_x$ complex was more stable than the $1\text{b}\text{-}\gamma\text{-CD}_x$ complex because the two substituent groups in 1a could smoothly penetrate the upper rim of two $\gamma\text{-CD}_x$ units without steric interference. When the residues obtained following concentration of the D_2O – $\text{DMSO-}d_6$ solution [2:3 (v/v)] were dissolved in CDCl_3 , only 1a could be separated from the $1\text{a}\text{-}\gamma\text{-CD}_x$ complex [Figure 6f; sample (C) in Scheme 1]. In contrast, 1c was extracted using larger amounts of $\gamma\text{-CD}_x$ ($[\gamma\text{-CD}_x]/[1] = 4, 1\text{a:1b:1c} = 2:16:82$), and only 1c could be separated when the amount of $\gamma\text{-CD}_x$ was increased further ($[\gamma\text{-CD}_x]/[1] = 8, 1\text{a:1b:1c} = 0:0:100$) (Table S2, SI, and Figure 6d,e) following the addition of DMSO [$\text{D}_2\text{O:DMSO-}d_6 = 2:1$ (v/v)]. These results suggested that the $1\text{c}\text{-}\gamma\text{-CD}_x$ complex was not as stable as the 1a and $1\text{b}\text{-}\gamma\text{-CD}_x$ complexes because the two substituent

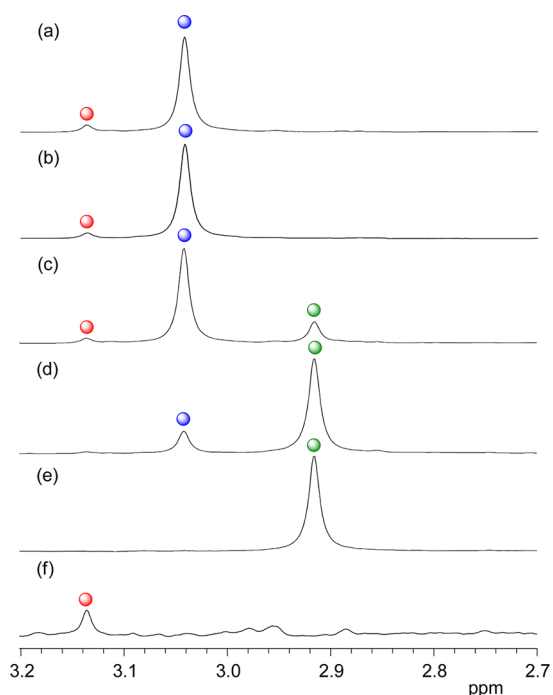


Figure 6. ^1H NMR spectra (400 MHz, CDCl_3) of the precipitates (a–e) obtained by the addition of DMSO [(a)–(c): D_2O – $\text{DMSO-}d_6$ = 1:1 (v/v), (d–e): D_2O – $\text{DMSO-}d_6$ = 2:1 (v/v); sample (D) in Scheme 1] and (f) the residue obtained after concentration of the solution obtained by the addition of DMSO [CDCl_3 ; sample (C) in Scheme 1]. $[\gamma\text{-CDx}]/[\mathbf{1}]$ = (a) 1.0, (b) 1.5, (c) 2.0, (d) 4.0, (e) 8.0, and (f) 1.5 (red ●, **1a**; blue ●, **1b**; green ●, **1c**). All spectra were recorded at 25 °C.

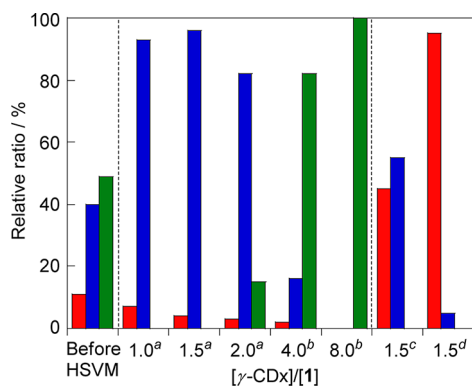


Figure 7. Relative ratios of **1** prior to the HSVM treatment and the ratios of **1** in the CDCl_3 and D_2O – $\text{DMSO-}d_6$ solutions obtained from the precipitates and the solutions, respectively, following the addition of DMSO. $[\gamma\text{-CDx}]/[\mathbf{1}]$ = 1.0, 1.5, 2.0, 4.0, and 8.0. (a) the precipitate obtained following the addition of DMSO [D_2O : $\text{DMSO-}d_6$ = 1:1 (v/v); sample (D) in Scheme 1], (b) the precipitate obtained following the addition of DMSO [D_2O : $\text{DMSO-}d_6$ = 2:1 (v/v); sample (D) in Scheme 1], (c) the solution following the addition of DMSO [D_2O : $\text{DMSO-}d_6$ = 1:1 (v/v); sample (C) in Scheme 1], (d) the solution following the addition of DMSO [D_2O : $\text{DMSO-}d_6$ = 2:3 (v/v); sample (C) in Scheme 1], (red bar, **1a**; blue bar, **1b**; green bar, **1c**).

groups of **1c** could not simultaneously penetrate the upper rim of two $\gamma\text{-CDx}$ units as a consequence of steric interference.

Characterization of $1\bullet\gamma\text{-CDx}$ Complexes. To develop a better understanding of the observed selectivity levels, the actual formation of the $1\bullet\gamma\text{-CDx}$ complexes was investigated in greater detail. When $[\gamma\text{-CDx}]/[\mathbf{1}]$ = 1.0–2.0, several new peaks

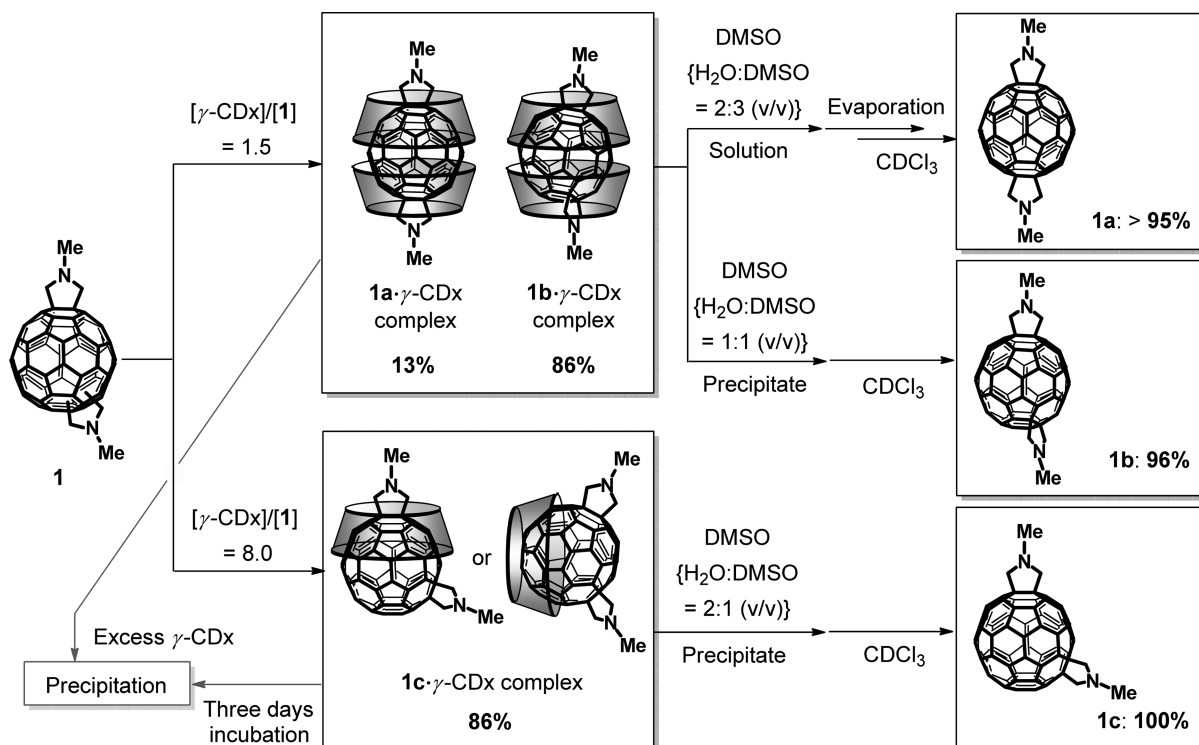
appeared in the ^1H NMR spectra of the $1\text{-}\gamma\text{-CDx}$ mixtures [Figure 2b–d; sample (A) in Scheme 1], which were attributed to the **1a** and **1b** $\bullet\gamma\text{-CDx}$ complexes. These new peaks were similar to those observed in the pristine $\text{C}_{60}\bullet\gamma\text{-CDx}$ complex. The stoichiometries of the complexes of **1a** and **1b** with $\gamma\text{-CDx}$ were determined to be 1:1.8–2.1 (Table 1) from the peak

Table 1. Stoichiometries of $1\bullet\gamma\text{-CDx}$ Complexes in D_2O Solution Following the HSVM Treatment

$[\gamma\text{-CDx}]/[\mathbf{1}]$	1	$\gamma\text{-CDx}$
1.0	1	1.8
2.0	1	2.1

intensities of the sum of **1a** and **1b** and $\gamma\text{-CDx}$. These results indicated that the **1a** and **1b** $\bullet\gamma\text{-CDx}$ complexes were 1:2 complexes (Scheme 2). The formation of 1:2 complexes was also supported by the results obtained from electrospray ionization mass spectroscopy (ESI-MS). When an aqueous solution of the **1a** and **1b** $\bullet\gamma\text{-CDx}$ complexes was subjected to ESI-MS ($[\gamma\text{-CDx}]/[\mathbf{1}]$ = 1.5, H_2O),¹⁷ a weak peak appeared at 3449.97, which was assigned to $[1:2\ \mathbf{1}\bullet\gamma\text{-CDx}\ \text{complex} + \text{Na}]^+$ (Figure 8). In contrast, when $[\gamma\text{-CDx}]/[\mathbf{1}]$ = 8.0, no assignable peak appeared for $\gamma\text{-CDx}$ in the **1c** $\bullet\gamma\text{-CDx}$ complex [Figure 2f; sample (A) in Scheme 1], suggesting that **1c** did not form a 1:2 complex in the same way as **1a** and **1b** (Scheme 2). Although it was assumed that **1c** formed a large self-aggregate, this hypothesis was inconsistent with the data because a sharp absorption band at 246 nm was observed in the UV–vis absorption spectrum (Figure 4, orange line) and the average particle size was determined to be 1.5 nm by dynamic light scattering (DLS) measurements (Table S3, SI). The lack of a separated peak assignable to $\gamma\text{-CDx}$ in the ^1H NMR spectrum of the **1c** $\bullet\gamma\text{-CDx}$ complex could be a consequence of the coalescence with peaks from the free $\gamma\text{-CDx}$ because the complexation-decomplexation exchange rate could have been faster than the ^1H NMR time-scale. Changes in the chemical shifts of $\gamma\text{-CDx}$ from those of the free $\gamma\text{-CDx}$ were negligible because of the large excess of free $\gamma\text{-CDx}$. The absence of an intermolecular hydrogen bonding network between the two $\gamma\text{-CDx}$ units in the **1c** $\bullet\gamma\text{-CDx}$ 1:1 complex could have been responsible for the fast exchange rate and led to the lability of the **1c** $\bullet\gamma\text{-CDx}$ complex by the addition of DMSO. The aqueous solution of the **1c** $\bullet\gamma\text{-CDx}$ complex underwent precipitation within 3 days at room temperature.

Stabilities of $1\bullet\gamma\text{-CDx}$ Complexes in Water. Comparative molecular dynamics (MD) simulations were performed for the **1a**, **1b**, and **1c** $\bullet\gamma\text{-CDx}$ complexes in water to evaluate the effects of the structural changes in the fullerene derivatives on the stabilities of the complexes. Initial structure of the complex is taken from a crystal structure,^{13b} where the fullerene derivative encapsulated by two $\gamma\text{-CDx}$ units. The number of hydrogen bonding interactions between the two $\gamma\text{-CDx}$ units (N_{hb}) was monitored throughout the MD simulations to evaluate the stabilities of the complexes. Unlike in the crystal structure, two $\gamma\text{-CDx}$ units do not always keep the hydrogen bonding to each other because of possible hydrogen bonding to surrounding water molecules in addition to thermal fluctuation. Indeed, the time period of no hydrogen bonding between $\gamma\text{-CDx}$ units was detected even in the most stable **1a** $\bullet\gamma\text{-CDx}$ complex in the course of MD simulations, showing a large fluctuation in the hydrogen bonding interaction between the $\gamma\text{-CDx}$ units. Figure 9 plots the block-averaged N_{hb} over every 0.5

Scheme 2. Schematic Illustration of the $1\bullet\gamma$ -CDx Complexes under the Low and High Concentrations of γ -CDx^a

^aPercentages represent the relative ratios.

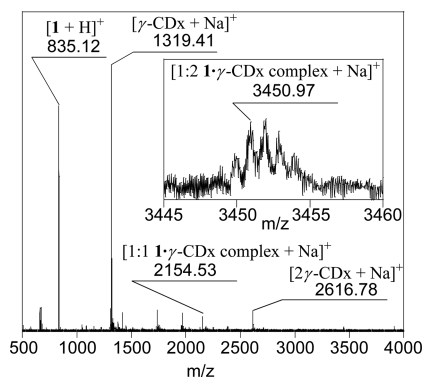


Figure 8. ESI-MS spectra of the **1a** and **1b**• γ -CDx complexes ($[\gamma\text{-CDx}]/[\mathbf{1}] = 1.5$, H_2O).

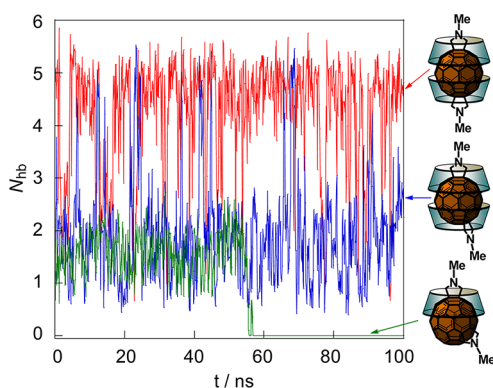


Figure 9. Time evolution of the number of hydrogen bonding (N_{hb}) between γ -CDx units in each complex. Red line, **1a**• γ -CDx complex; blue line, **1b**• γ -CDx complex; and green line, **1c**• γ -CDx complex.

ns. A clear difference is detected among the three γ -CDx complexes. Although the **1c**• γ -CDx complex retained a few hydrogen bonding interaction during the first 55 ns, one γ -CDx unit eventually dissociated from the complex. Once dissolved into water, the γ -CDx unit did not come back to the complex throughout the MD simulation, whereas the other γ -CDx unit remained in contact with the fullerene derivative. This simulation was consistent with the experimental observations. In contrast, the **1a**• γ -CDx complex retained 4.2 hydrogen bonding interactions on average, whereas the **1b**• γ -CDx complex had 1.9 hydrogen bonding interactions on average. Although these numbers were relatively sensitive to the choice of the parameters selected to define the hydrogen bonding interactions, the qualitative difference between the complexes regarding the stabilities of the hydrogen bonding interactions was clearly evident. As shown in Figure S8, SI, a time course of the calculated cohesive energy provided the same information as that provided from a plot of the number of hydrogen bonding interactions (Figure 9). Figures 10 show three typical snapshots of the MD simulations. In the case of $N_{\text{hb}} \sim 4-5$, two γ -CDx units associated to form a closed capsule, although the opening of a mouth like structure occurred when $N_{\text{hb}} \sim 1-2$. The two *N*-acylated pyrrolidine moieties of the fullerenes clearly affected the orientation of the associated γ -CDx. Thus, two γ -CDx units in the **1b**• γ -CDx complex simply existed in a fully closed association, exposing their hydroxy groups toward the water. To completely and effectively assess the thermal stabilities of the γ -CDx complexes, a free energy calculation would be required, and this represents a future piece of work. The differences detected in the structures of the complexes as well as in the number of hydrogen bonding interaction, however, strongly suggested that the **1a**• γ -CDx complex was more stable than the **1b**• γ -CDx complex.

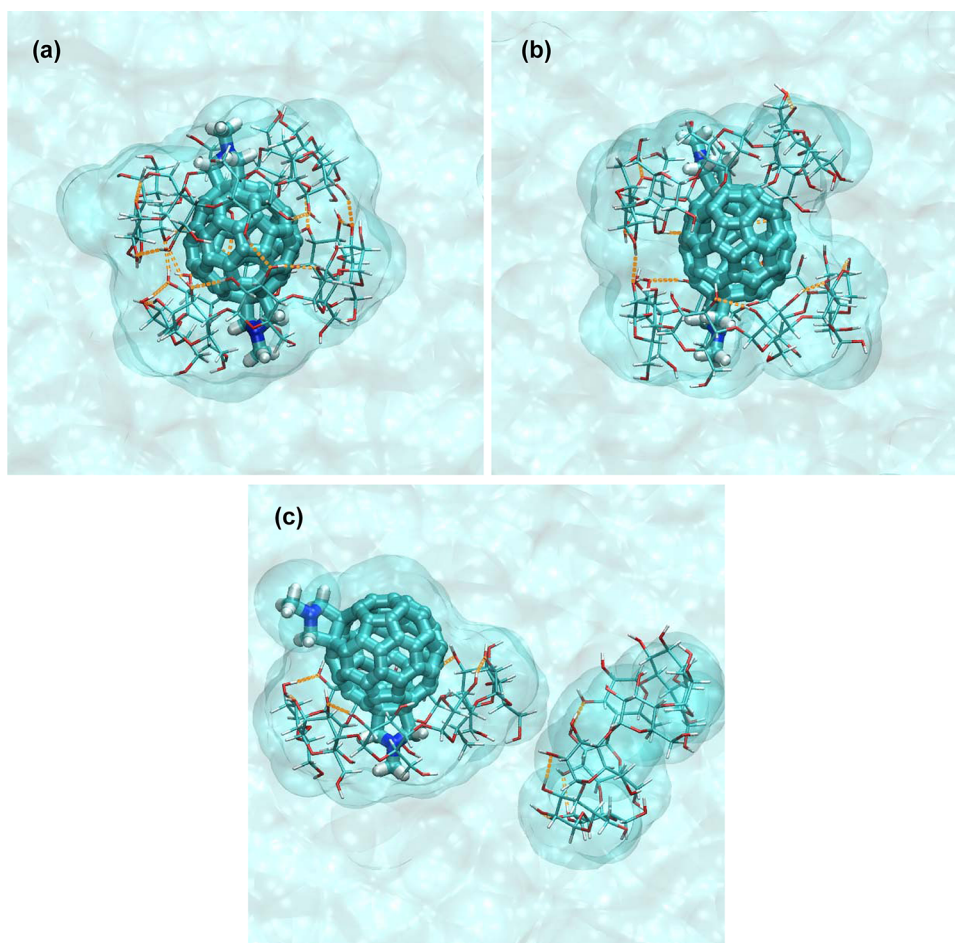


Figure 10. Snapshots of solvated γ -CDx complexes from MD simulations. (a) $1a \bullet \gamma$ -CDx, (b) $1b \bullet \gamma$ -CDx, and (c) $1c \bullet \gamma$ -CDx complexes. The hydrogen bonding interactions within the γ -CDx are indicated by the orange dashed lines. Water is depicted with a transparent surface. The carbons are shown in cyan, oxygens in red, nitrogens in blue, and hydrogens in white.

CONCLUSION

In conclusion, although γ -CDx formed 2:1 complexes with **1a** and **1b** in D_2O containing NaOD under low concentrations of γ -CDx the selectivity for the formation of the complex with γ -CDx was low. However, only **1b** precipitated out readily on the addition of DMSO because the stability of the $1b \bullet \gamma$ -CDx 1:2 complex was lower than that of the $1a \bullet \gamma$ -CDx 1:2 complex. The difference in the stabilities of the **1a** and $1b \bullet \gamma$ -CDx complexes was attributed to the larger number of hydrogen bonding interactions between the two γ -CDx units in the $1a \bullet \gamma$ -CDx complex, compared with the number of interactions in the $1b \bullet \gamma$ -CDx complex as shown by the MD simulations. The filtrate contained a high proportion of the $1a \bullet \gamma$ -CDx 1:2 complex. In contrast, **1c** formed a 1:1 complex with γ -CDx that dissolved in D_2O containing NaOD in the presence of a large amount of γ -CDx. MD simulations indicated that the difficulties encountered with the multipoint-hydrogen bonding interactions between two γ -CDx units resulted in the formation of a 1:1 complex as opposed to a 1:2 complex. The presence of an excess of free γ -CDx, however, effectively lowered the solubilities of the **1a** and $1b \bullet \gamma$ -CDx complexes in D_2O containing NaOD. Furthermore, the $1c \bullet \gamma$ -CDx 1:1 complex readily decomposed to give only **1c** as the precipitate following the addition of DMSO to the solution. The selectivity was therefore led by a competition between the stabilities and solubilities of the complexes in D_2O containing NaOD and

DMSO. By forming a complex with γ -CDx, we succeeded in the regioselective separation of **1a–c**. These compounds are precursors of the cationic bis-*N,N*-dimethylfulleropyrrolidinium salts which have received considerable attention because of their potential applications in medicinal chemistry. Further studies for other fullerene derivatives are currently underway in our laboratories.

EXPERIMENTAL SECTION

Materials. γ -CDx was purchased from the Aldrich Chemical Co., Inc. (Milwaukee, WI). Compound **1** was prepared according to a method previously described in the literature.¹⁸ The 1H NMR and mass spectra of **1** are shown in Figures S2a and S3, SI.

UV–Vis Absorption Spectroscopy. All experiments were performed at 25 °C and a 1 mm cell was used.

1H NMR Spectroscopy. We used 3-(trimethylsilyl)propionic-2,2,3,3- d_4 acid sodium salt as an internal standard.

Dynamic Light Scattering (DLS) Analysis. The hydrodynamic diameters of the **1**– γ -CDx mixtures were measured on an instrument for electrophoretic light scattering with a laser Doppler system (Zetasizer Nano ZS, Malvern Instruments Ltd., Malvern, UK).

Preparation of the C_{60} – γ -CDx Complex. A mixture of **1** (5.00 mg, 5.99 μ mol) and γ -CDx ($[\gamma\text{-CDx}]/[\mathbf{1}] = 1.0, 1.5, 2.0, 4.0, \text{ or } 8.0$) was placed in an agate capsule together with two agate mixing balls and mixed vigorously at 1800 rpm for 20 min using a high-speed vibration mill (MM200, Retsch Co. Ltd., Haan, Germany). The mixture was then dissolved in D_2O containing 1 mM NaOD (1.5 mL)¹⁵ to produce a brown emulsion. The D_2O solution of **1**– γ -CDx mixture and the

precipitate of nondisperse **1** were separated by centrifugation (18000×g, 20 min, 25 °C). Following the measurement of the UV–vis absorption and ¹H NMR spectra, DMSO ([γ-CDx]/[**1**] = 1.0–2.0; 1.0 mL, [γ-CDx]/[**1**] = 4.0–8.0; 0.5 mL) was added to the D₂O solution (1.0 mL) leading to the precipitation of **1**. The precipitate was then dissolved in CDCl₃ for analysis by ¹H NMR spectroscopy.

Molecular Dynamics (MD) Simulations. Molecular dynamics simulations were performed at constant pressure (1 atm) and temperature (298 K) using the NAMD software.¹⁹ The CHARMM force field (C36)^{20,21} was used to model the γ-CDx and fullerenes, whereas the fractional charges of the fullerene derivatives were estimated by molecular orbital calculations at the B3LYP/6-31G(d) level with the Merz–Singh–Kollman scheme.²² The TIP3P model was employed for water.²³ Initial structures of the **1a**, **1b**, and **1c**•γ-CDx complexes were taken from the crystal structure^{13b} with the modifications needed for the fullerene derivatives. For the **1c**•γ-CDx complex in particular, the fullerene derivative was slightly moved and rotated within the γ-CDx cage to prevent a poor physical contact between the γ-CDx units and the fullerene derivative. The complexes were placed in a water box of about 40 Å in length. The Coulomb interaction was calculated using the particle mesh Ewald method.²⁴ All bonds involving hydrogen atoms were constrained to their equilibrium lengths based on the SHAKE/RATTLE algorithm.²⁵ The time step size was 2 fs. Following an equilibration MD run of 20 ns, a 60 ns-production MD run was carried out for each system. For the analysis of the hydrogen bonding interactions between the γ-CDx units, the two hydroxyl groups between the different γ-CDx units were considered to be hydrogen-bonded only if their interoxygen distance was <3.2 Å, and simultaneously the angle between the O–O axis and one of the O–H bonds was 30°.

■ ASSOCIATED CONTENT

● Supporting Information

Supporting Figures (S1–S7) and Tables (S1–S3). This material is available free of charge via the Internet at <http://pubs.acs.org>.

■ AUTHOR INFORMATION

Corresponding Author

*E-mail: aikeda@ms.naist.jp.

Notes

The authors declare no competing financial interest.

■ ACKNOWLEDGMENTS

This work was supported by the Grant-in-Aid for Challenging Exploratory Research (No. 24655128) from the Japan Society for the Promotion of Science (JSPS). W.S. is grateful to Dr. S. Tsuzuki for helpful discussion.

■ REFERENCES

- (1) (a) Imahori, H.; Sakata, Y. *Adv. Mater.* **1997**, *9*, 537–546. (b) Echegoyen, L.; Echegoyen, L. E. *Acc. Chem. Res.* **1998**, *31*, 593–601. (c) Bottari, G.; de la Torre, G.; Guldi, D. M.; Torres, T. *Chem. Rev.* **2010**, *110*, 6768–6816.
- (2) (a) Martín, N.; Sánchez, L.; Illescas, B.; Pérez, I. *Chem. Rev.* **1998**, *98*, 2527–2547. (b) Da Ros, T.; Prato, M. *Chem. Commun.* **1999**, 663–669. (c) Bakry, R.; Vallant, R. M.; Najam-ul-Haq, M.; Rainer, M.; Szabo, Z.; Huck, C. W.; Bonn, G. K. *Int. J. Nanomed.* **2007**, *2*, 639–649. (d) Bosi, S.; Da Ros, T.; Spalluto, G.; Prato, M. *Eur. J. Med. Chem.* **2003**, *38*, 913–923. (e) Yano, S.; Hirohara, S.; Obata, M.; Hagiya, Y.; Ogura, S.; Ikeda, A.; Kataoka, H.; Tanaka, M.; Joh, T. *J. Photochem. Photobiol., C* **2011**, *12*, 46–67.
- (3) (a) Thilgen, C.; Diederich, F. *Chem. Rev.* **2006**, *106*, 5049–5135. (b) Nakamura, Y.; Kato, S. *Chem. Rec.* **2011**, *11*, 77–94.
- (4) (a) Prato, M.; Maggini, M. *Acc. Chem. Res.* **1998**, *31*, 519–526. (b) Lu, Q.; Schuster, D. L.; Wilson, S. R. *J. Org. Chem.* **1996**, *61*, 4764–4768. (c) Kordatos, K.; Bosi, S.; Da Ros, T.; Zambon, A.; Lucchini, V.;

Prato, M. *J. Org. Chem.* **2001**, *66*, 2802–2808. (d) Nakamura, Y.; Okawa, K.; Nishimura, T.; Yashima, E.; Nishimura, J. *J. Org. Chem.* **2003**, *68*, 3251–3257. (e) Nishimura, T.; Tsuchiya, K.; Ohsawa, S.; Maeda, K.; Yashima, E.; Nakamura, Y.; Nishimura, J. *J. Am. Chem. Soc.* **2004**, *126*, 11711–11717.

(5) (a) Nierengarten, J.-F.; Gramlich, V.; Cardullo, D.-C. F.; Diederich, F. *Angew. Chem., Int. Ed. Engl.* **1996**, *35*, 2101–2103. (b) Nierengarten, J.-F.; Habicher, T.; Kessinger, R.; Cardullo, F.; Diederich, F.; Gramlich, V.; Gisselbrecht, J. P.; Boudon, C.; Gross, M. *Helv. Chim. Acta* **1997**, *80*, 2238–2276. (c) Taki, M.; Sugita, S.; Nakamura, Y.; Kasashima, E.; Yashima, E.; Okamoto, Y.; Nishimura, J. *J. Am. Chem. Soc.* **1997**, *119*, 926–932. (d) Ishi-i, T.; Nakashima, K.; Shinkai, S. *Chem. Commun.* **1998**, 1047–1048. (e) Ishi-i, T.; Nakashima, K.; Shinkai, S.; Ikeda, A. *J. Org. Chem.* **1999**, *64*, 984–990. (f) Bourgeois, J.-P.; Echegoyen, L.; Fibbioli, M.; Pretsch, E.; Diederich, F. *Angew. Chem., Int. Ed.* **1998**, *37*, 2118–2121. (g) Sergeev, S.; Schär, M.; Seiler, P.; Lukoyanova, O.; Echegoyen, L.; Diederich, F. *Chem.—Eur. J.* **2005**, *11*, 2284–2294. (h) Qian, W.; Rubin, Y. *Angew. Chem., Int. Ed.* **1999**, *38*, 2356–2360. (i) Riala, M.; Chronakis, N. *Org. Lett.* **2011**, *13*, 2844–2847.

(6) Zhang, S.; Lukoyanova, O.; Echegoyen, L. *Chem.—Eur. J.* **2006**, *12*, 2846–2853.

(7) (a) Suzuki, T.; Nakashima, K.; Shinkai, S. *Chem. Lett.* **1994**, 699–702. (b) Atwood, J. L.; Koutsantonis, G. A.; Raston, C. L. *Nature* **1994**, *368*, 229–231.

(8) (a) Komatsu, N. *Org. Biomol. Chem.* **2003**, *1*, 204–209. (b) Stefankiewicz, A. R.; Tamanini, E.; Pantos, G. D.; Sanders, J. K. M. *Angew. Chem., Int. Ed.* **2011**, *50*, 5724–5727.

(9) (a) Kunderát, O.; Káš, M.; Tkadlecová, M.; Lang, K.; Cvačka, J.; Stibor, I.; Lhoták, P. *Tetrahedron Lett.* **2007**, *48*, 6620–6623. (b) Kawauchi, T.; Kitaura, A.; Kawauchi, M.; Takeichi, T.; Kumaki, J.; Iida, H.; Yahima, E. *J. Am. Chem. Soc.* **2010**, *132*, 12191–12193.

(10) (a) Shoji, Y.; Tashiro, K.; Aida, T. *J. Am. Chem. Soc.* **2004**, *126*, 6570–6571. (b) Haino, T.; Fukunaga, C.; Fukazawa, Y. *Org. Lett.* **2006**, *8*, 3545–3548. (c) Calvaresi, M.; Zerbetto, F. *Nanoscale* **2011**, *3*, 2873–2881.

(11) Ikeda, A. In *Encyclopedia of Nanoscience and Nanotechnology*; Nalwa, H. S., Ed.; American Scientific Publishers: Stevenson Ranch, CA, 2011; Vol. 23, pp 329–347 and references cited therein.

(12) (a) Andersson, T.; Nilsson, K.; Sundahl, M.; Westman, G.; Wennerström, O. *J. Chem. Soc., Chem. Commun.* **1992**, 604–606. (b) Komatsu, K.; Fujiwara, K.; Murata, Y.; Braun, T. *J. Chem. Soc., Perkin Trans. 1* **1999**, 2963–2966.

(13) (a) Ikeda, A.; Genmoto, T.; Maekubo, N.; Kikuchi, J.; Akiyama, M.; Mochizuki, T.; Kotani, S.; Konishi, T. *Chem. Lett.* **2010**, *39*, 1256–1257. (b) Ikeda, A.; Aono, R.; Maekubo, N.; Katao, S.; Kikuchi, J.; Akiyama, M. *Chem. Commun.* **2010**, 47, 12795–12797.

(14) (a) Mashino, T.; Nishikawa, D.; Takahashi, K.; Usui, N.; Yamori, T.; Seki, M.; Endo, T.; Mochizuki, M. *Bioorg. Med. Chem. Lett.* **2003**, *13*, 4395–4397. (b) Pastorin, G.; Marchesan, S.; Hoebeke, J.; Da Ros, T.; Ehret-Sabatier, L.; Briand, J.-P.; Prato, M.; Bianco, A. *Org. Biomol. Chem.* **2006**, *4*, 2556–2562.

(15) Compound **1** is protonated in weakly acidic solution because **1** has two tertiary amines. After the protonation, **1**⁺ or **1**²⁺ may dissolve in D₂O by themselves or a formation of water-soluble micelles. To avoid the protonation of **1**, we used D₂O containing 1.0 mM NaOD as an extracting solvent.

(16) We attempted that the residue obtained after concentration of the D₂O solution were dissolved directly in CDCl₃ using ultrasonication but failed. The reason is expected because the **1**•γ-CDx complexes in the residue has a hydrophilic surface.

(17) By ESI-MS spectrometry, peaks for the 1:2 **1**•γ-CDx complexes were not observed in D₂O containing 1.0 mM NaOD. Therefore, we used H₂O as a solvent.

(18) Pasimeni, L.; Hirsch, A.; Lamparth, I.; Herzog, A.; Maggini, M.; Prato, M.; Corvaja, C.; Scorrano, G. *J. Am. Chem. Soc.* **1997**, *119*, 12896–12901.

- (19) Phillips, J.; Braun, R.; Wang, W.; Gumbart, J.; Tajkhorshid, E.; Villa, E.; Chipot, C.; Skeel, R.; Kale, L.; Schulten, K. *J. Comput. Chem.* **2005**, *26*, 1781–1802.
- (20) Guvench, O.; Mallyosyula, S.; Raman, E. P.; Hatcher, E.; Vanommeslaeghe, K.; Foster, T. J.; Jamison, F. W., II; MacKerell, A. D. *J. Chem. Theory Comput.* **2011**, *7*, 3162–3180.
- (21) Vanommeslaeghe, K.; Hatcher, E.; Acharya, C.; Kundu, S.; Zhong, S.; Shim, J.; Darian, E.; Guvench, O.; Lopes, P.; Vorobyov, I.; Mackerell, A. D. *J. Comput. Chem.* **2010**, *31*, 671–690.
- (22) Singh, U. C.; Kollman, P. A. *J. Comput. Chem.* **1984**, *5*, 129–145.
- (23) Jorgensen, W. L.; Chandrasekhar, J.; Madura, J. D.; Impey, R. W.; Klein, M. L. *J. Chem. Phys.* **1983**, *79*, 926–935.
- (24) Essmann, U.; Perera, L.; Berkowitz, M. L.; Darden, T.; Lee, H.; Pedersen, L. G. *J. Chem. Phys.* **1995**, *103*, 8577–7593.
- (25) Ryckaert, J.; Ciccotti, G.; Berendsen, H. J. *Comput. Phys.* **1977**, *23*, 327–341.